

The decay $\tau \rightarrow 3\pi\nu_\tau$ as a probe of the mechanism of dynamical chiral symmetry breaking

Luca Girlanda and Jan Stern

*Division de Physique Théorique, Institut de Physique Nucléaire
F-91406 Orsay Cedex
France*

ABSTRACT: The decays $\tau \rightarrow 3\pi + \nu_\tau$ are analyzed at one loop order in the framework of Generalized Chiral Perturbation Theory, in order to test the sensitivity to the size of spontaneous chiral symmetry breaking parameters, contained in the S-wave. The latter, due to a kinematical suppression, at threshold, of the P-wave, is relatively large enough to be detectable at high energy machines, through azimuthal left-right asymmetries. This quantity (for the $\pi^-\pi^-\pi^+$ mode), integrated from threshold to $Q^2 = 0.35 \text{ GeV}^2$, varies from $(17 \pm 3)\%$ in the standard case of large condensate up to $(40 \pm 5)\%$ in the extreme case of tiny condensate. The feasibility of such measurement at high luminosity colliders (*e.g.* CLEO) is discussed. This method provides a completely independent cross-check of forthcoming experimental determination of the quark condensate, based on low energy $\pi\pi$ scattering.

KEYWORDS: Nonperturbative Effects, QCD, Chiral Lagrangians, Weak Decays.

Contents

1. Introduction	1
2. The generalized expansion of the $SU(2) \times SU(2)$ lagrangian	3
3. Kinematics	7
4. The hadronic matrix element in $G_\chi PT$	10
5. Connection with low-energy $\pi\pi$ observables	13
6. Structure functions and azimuthal asymmetries	15
7. The size of the spin 0 spectral function	23
8. Concluding remarks	25

1. Introduction

The mechanism of dynamical (chiral) symmetry breaking and the identification of its experimental signatures is one of the central subjects in modern particle theory. The problem is to understand non-perturbative alternatives to the spontaneous symmetry breaking triggered by elementary weakly coupled scalar fields, whose nature is essentially perturbative. The problem arises at different energy scales characteristic of the Standard Model and its extensions. At low energy QCD, $E < 1$ GeV, the nonperturbative dynamical breaking of chiral symmetry (DBCHS) is unavoidable, since QCD does not contain elementary weakly coupled scalars. Yet, the mechanism of DBCHS, in particular the role and importance of the quark-antiquark condensate $\langle \bar{q}q \rangle$, are not understood theoretically and they remain poorly known experimentally [1]. At higher energy scales $E \sim (10^2 - 10^3)$ GeV, a dynamical electroweak symmetry breaking is of interest as a possible alternative to an elementary weakly coupled light scalar Higgs protected by Supersymmetry. This alternative assumes the existence of a new QCD-like (confining) gauge theory which breaks dynamically its chiral symmetry at a scale $\Lambda_{sb} \sim (2 - 3)$ TeV. The Goldstone bosons would then transmit this DBCHS to the electroweak sector by the Higgs mechanism (for a recent review see Ref. [2]) . In order to make such a scenario specific and to investigate its

consistency with electroweak precision measurements at low energies ($E \ll \Lambda_{\text{sb}}$), one usually takes the presumed mechanism of DBCHS in QCD as a prototype, assuming in addition, a simple dependence on the scale and on the number of (techni-)colors N_c and of light (techni-)fermion dublets N_D [3]. If the mechanism of DBCHS in QCD-like theories turned out to be different from the general expectation (concerning *e.g.* the role of chiral condensates in a dynamical generation of fermion masses, the possible existence of new phase transitions as a function of N_c and N_D and their influence on the spectrum of bound states, ...), the estimates of oblique and vertex corrections to the tree level Standard Model [3] could be substantially modified¹. Below the scale Λ_{sb} , at which new degrees of freedom (“techni-hadrons”) start to be visible, the precision tests of models of dynamical electroweak symmetry breaking can hardly be dissociated from the investigation of the mechanism of DBCHS in low energy QCD. The importance of dedicated experimental tests of the latter for the low-energy QCD phenomenology as it appears *e.g.* in the calculation of weak matrix elements, determination of CKM matrix elements or estimates of running light quark masses, has been often mentioned. (It has, for instance, been pointed out [5] that if the condensate $\langle \bar{q}q \rangle$ does not dominate the expansion of symmetry breaking effects, the SM evaluation of ϵ'/ϵ could lead to a significantly higher value than in the case of the standard scenario of DBCHS). Actually, model independent tests of the role of $\langle \bar{q}q \rangle$ in QCD are of more fundamental and larger interest: they may concern the mechanism of dynamical electroweak symmetry breaking at the TeV scale and the problem of the origin of masses.

The purpose of this paper is to propose a new test of the importance of the quark condensate in the mechanism of chiral symmetry breaking in QCD. The experimental signature of this mechanism can be systematically investigated using the technique of the effective theory [6], and its low energy expansion - χ PT [7, 8]. The standard version of this expansion (S χ PT) assumes a dominant role of $\langle \bar{q}q \rangle$ that is a small deviation from the Gell-Mann–Oakes–Renner (GOR) relation [9]. If the condensate is less important the standard low energy expansion of the same effective Lagrangian has to be modified leading to the Generalized χ PT (G χ PT). The latter is the proper framework for measuring $\langle \bar{q}q \rangle$ since it makes no assumptions on its size nor about the deviation from the GOR relation².

In this way the low energy $\pi\pi$ scattering in the S-wave has been identified as being particularly sensitive to $\langle \bar{q}q \rangle$ [10, 11, 12]. The corresponding experimental tests now become possible, due to *i*) the control of the precision of χ PT which now reaches two-loop accuracy and is able to produce a precise prediction of the standard

¹A remark in this sense has been recently made in Ref. [4], concerning the value and the sign of the parameter L_{10} .

²The quark condensate by itself is not an observable quantity. What can be actually measured is the renormalization group invariant product $\hat{m}\langle \bar{u}u + \bar{d}d \rangle_{\hat{m}=0}$ in units of $F_\pi^2 M_\pi^2$, that is precisely the deviation from the GOR relation.

scenario [7, 13] and on the other hand to interpret any substantial deviation from this prediction in terms of unexpectedly weak values of quark condensate [11]; *ii*) the fact that the needed precision (5 % or better for the S-wave scattering length) can be reached: in the on-going $\pi^+ - \pi^-$ atoms lifetime measurement at CERN [14], in the new precise K_{e4}^+ experiments, E865 at BNL [15] and, in the near future, at the Frascati ϕ factory Da ϕ ne (with the KLOE detector) [16].

In view of the importance of this issue it is interesting to identify independent sources of similar experimental information. In this paper a proposal is elaborated in detail concerning the decays $\tau \rightarrow 3\pi + \nu_\tau$ at low invariant mass of the hadronic system $Q^2 < 0.35 \text{ GeV}^2$. The S-wave is proportional to the divergence of the axial current and it measures the importance of chiral symmetry breaking away from the pion pole. However, when considering this process in χ PT, one is faced with two main difficulties: *i*) the smallness of the branching ratio in the threshold region, which is the only domain where χ PT is applicable, and *ii*) the chiral suppression of the S-wave compared to the P-wave (which, moreover is enhanced by the a_1 resonance). The former problem now becomes less stringent, as pointed out in Ref. [17], thanks to the large statistics already accumulated in the present machines and to the improvements expected for the near future (for a review see Ref. [18]). As for the latter, it turns out (cfr. Ref. [19]) that the P-wave, although dynamically dominant, is kinematically suppressed, near the threshold, compared to the S-wave. These two facts together allow the S-wave contribution to show up in a clean and detectable way. The plan of the paper is as follows. In Section 2 the generalized $\text{SU}(2) \times \text{SU}(2)$ chiral lagrangian is constructed and renormalized at $\mathcal{O}(p^4)$ level. In Section 3 we will recall the kinematics of the $\tau \rightarrow 3\pi\nu_\tau$ decays and the definitions of the structure functions, following Ref. [19]. In Section 4 we compute the hadronic matrix element at one-loop of $\text{G}\chi\text{PT}$, and in Section 5 we discuss the relation with $\pi\pi$ observables. The numerical results for the structure functions and their dependence on the quark condensate are shown in Section 6. In particular we will focus on the azimuthal asymmetries, which are very straightforward observables to extract experimentally. In Section 7 we discuss the relevance of our results for the QCD sum rules used to extract the quark masses. Finally we will summarize with some concluding remarks in Section 8.

2. The generalized expansion of the $\text{SU}(2) \times \text{SU}(2)$ lagrangian

χ PT is an effective theory having as degrees of freedom only the lowest energy excitations of the spectrum of QCD, that is the Goldstone bosons. In the case of $\text{SU}(2) \times \text{SU}(2)$ chiral symmetry these are the pion fields $\pi^j(x)$. They are collected in a unitary 2×2 matrix

$$U(x) = \exp \left[\frac{i\pi^j(x)\tau^j}{F} \right], \quad j = 1, 2, 3, \quad (2.1)$$

with τ^j the Pauli matrices, and F the pion decay constant in the chiral limit. The external sources coupled to the vector, axial-vector, scalar and pseudoscalar quark currents are also represented by hermitian 2×2 matrices

$$v_\mu = \sum_{j=0}^3 v_\mu^j \tau^j, \quad a_\mu = \sum_{j=1}^3 a_\mu^j \tau^j, \quad s = \sum_{j=0}^3 s^j \tau^j, \quad p = \sum_{j=0}^3 p^j \tau^j. \quad (2.2)$$

The scalar source (which contains the quark mass matrix) and the pseudoscalar one are grouped in a complex matrix $\chi = s + ip$. The effective lagrangian is the most general one which is invariant under chiral symmetry and it contains an infinite number of terms; however, only a finite number of them will contribute at a given order of the low energy expansion. Since the latter is a simultaneous expansion in powers of momenta and quark masses, one has to establish a power counting rule for the quark masses. This can be done by considering the Taylor expansion of the pion mass squared in powers of quark mass (we will always stick to the isospin limit, $m_u = m_d = \hat{m}$)

$$M_\pi^2 = 2B\hat{m} + 4A\hat{m}^2 + \dots, \quad (2.3)$$

which is valid up to chiral logarithms. The coefficient of the linear term is proportional to the quark condensate,

$$B = - \lim_{\hat{m} \rightarrow 0} \frac{\langle \bar{u}u \rangle}{F^2} = - \lim_{\hat{m} \rightarrow 0} \frac{\langle \bar{d}d \rangle}{F^2}. \quad (2.4)$$

The standard assumption is that the latter is large enough for the first term to dominate the series (2.3), yielding the standard counting rule $\hat{m} \sim \mathcal{O}(p^2)$. In general, however, nothing prevents B to be much smaller than one may wish; in this case the counting rule has to be modified and, to be consistent, one has to consider formally B as a small parameter (notice that the parameter B has been removed from the definition of the matrix χ , compared to the standard notation). The generalized counting is then defined by

$$B \sim \hat{m} \sim \chi \sim \mathcal{O}(p), \quad (2.5)$$

so that the expansion of the effective lagrangian in $G\chi$ PT reads

$$\mathcal{L}^{\text{eff}} = \tilde{\mathcal{L}}^{(2)} + \tilde{\mathcal{L}}^{(3)} + \tilde{\mathcal{L}}^{(4)} + \dots \quad (2.6)$$

with

$$\tilde{\mathcal{L}}^{(d)} = \sum_{k+l+n=d} B^n \mathcal{L}_{(k,l)} \quad (2.7)$$

and $\mathcal{L}_{(k,l)}$ containing k derivatives and l powers of quark masses. Defining the covariant derivative as usual

$$D_\mu = \partial_\mu U - i[v_\mu, U] - i\{a_\mu, U\}, \quad (2.8)$$

and denoting by $\langle \dots \rangle$ the trace of the flavor 2×2 matrices, the leading, order $\mathcal{O}(p^2)$, lagrangian reads

$$\begin{aligned} \tilde{\mathcal{L}}^{(2)} = \frac{F^2}{4} \Big\{ & \langle D_\mu U^\dagger D^\mu U \rangle + 2B \langle U^\dagger \chi + \chi^\dagger U \rangle + A \langle (U^\dagger \chi)^2 + (\chi^\dagger U)^2 \rangle \\ & + Z^P \langle U^\dagger \chi - \chi^\dagger U \rangle^2 + h_0 \langle \chi^\dagger \chi \rangle + h'_0 (\det \chi + \det \chi^\dagger) \Big\}. \end{aligned} \quad (2.9)$$

Terms which would be of order $\mathcal{O}(p^4)$ in the standard counting are already present at the lowest order in the generalized case, reflecting the fact that the linear and the quadratic contribution in Eq. (2.3) can compete. Up to a given chiral order the $S\chi$ PT lagrangian is a subset of the $G\chi$ PT one. The last two terms are high energy counter terms, needed for the renormalization of the theory, but they will not appear in the expressions of matrix elements of pions on the mass shell. Using the equations of motion, field redefinitions, the identity

$$M^2 - M \langle M \rangle + \det M = 0 \quad (2.10)$$

valid for any 2×2 matrix M , and the fact that

$$D_\mu U^\dagger D^\mu U = \frac{1}{2} \langle D_\mu U^\dagger D^\mu U \rangle, \quad (2.11)$$

to absorb the redundant terms, we arrive at the following expressions for the $\tilde{\mathcal{L}}^{(3)}$ lagrangian³

$$\begin{aligned} \tilde{\mathcal{L}}^{(3)} = \frac{1}{4} F^2 \Big\{ & \xi^{(2)} \langle D_\mu U^\dagger D^\mu U (\chi^\dagger U + U^\dagger \chi) \rangle + \rho_1^{(2)} \langle (\chi^\dagger U)^3 + (U^\dagger \chi)^3 \rangle \\ & + \rho_2^{(2)} \langle (\chi^\dagger U + U^\dagger \chi) \chi^\dagger \chi \rangle + \rho_3^{(2)} \langle \chi^\dagger U - U^\dagger \chi \rangle \langle (\chi^\dagger U)^2 - (U^\dagger \chi)^2 \rangle \\ & + \rho_4^{(2)} \langle \chi^\dagger U + U^\dagger \chi \rangle \langle (\chi^\dagger U)^2 + (U^\dagger \chi)^2 \rangle + \rho_5^{(2)} \langle \chi^\dagger \chi \rangle \langle \chi^\dagger U + U^\dagger \chi \rangle \Big\}, \end{aligned} \quad (2.12)$$

and for $\tilde{\mathcal{L}}^{(4)} = \mathcal{L}_{(4,0)} + \mathcal{L}_{(2,2)} + \mathcal{L}_{(0,4)}$,

$$\begin{aligned} \mathcal{L}_{(4,0)} = & \frac{l_1}{4} \langle D_\mu U^\dagger D^\mu U \rangle^2 + \frac{l_2}{4} \langle D_\mu U^\dagger D_\nu U \rangle \langle D^\mu U^\dagger D^\nu U \rangle + l_5 \langle F_{\mu\nu}^R U F^{L,\mu\nu} U^\dagger \rangle \\ & + i \frac{l_6}{2} \langle F_{\mu\nu}^R D^\mu U D^\nu U^\dagger + F_{\mu\nu}^L D^\mu U^\dagger D^\nu U \rangle \\ & - \left(2h_2 + \frac{1}{2} l_5 \right) \langle F_{\mu\nu}^R F^{R,\mu\nu} + F_{\mu\nu}^L F^{L,\mu\nu} \rangle. \end{aligned} \quad (2.13)$$

$$\begin{aligned} \mathcal{L}_{(2,2)} = & \frac{1}{4} F^2 \Big\{ a_1 \langle D_\mu U^\dagger D^\mu U (\chi^\dagger \chi + U^\dagger \chi \chi^\dagger U) \rangle + a_2 \langle D_\mu U^\dagger U \chi^\dagger D^\mu U U^\dagger \chi \rangle \\ & + a_3 \langle D_\mu U^\dagger U (\chi^\dagger D^\mu \chi - D^\mu \chi^\dagger \chi) + D_\mu U U^\dagger (\chi D^\mu \chi^\dagger - D^\mu \chi \chi^\dagger) \rangle \end{aligned}$$

³The same lagrangian, up to and including $\mathcal{O}(p^4)$, has been found, independently, by Marc Knecht [20], to whom we are indebted for useful correspondence. Notice that in this reference different notations have been chosen for the pure source terms h'_0 and $h_{(2,2)}$.

$$\begin{aligned}
& +b_1 \langle D_\mu U^\dagger D^\mu U (\chi^\dagger U \chi^\dagger U + U^\dagger \chi U^\dagger \chi) \rangle \\
& +b_2 \langle D_\mu U^\dagger \chi D^\mu U^\dagger \chi + \chi^\dagger D_\mu U \chi^\dagger D^\mu U \rangle \\
& +b_3 \langle U^\dagger D_\mu \chi U^\dagger D^\mu \chi + D_\mu \chi^\dagger U D^\mu \chi^\dagger U \rangle \\
& +c_1 \langle D_\mu U^\dagger \chi + \chi^\dagger D_\mu U \rangle \langle D^\mu U^\dagger \chi + \chi^\dagger D^\mu U \rangle \\
& +c_2 \langle D_\mu \chi^\dagger U + U^\dagger D_\mu \chi \rangle \langle D^\mu U^\dagger \chi + \chi^\dagger D^\mu U \rangle \\
& +c_3 \langle D_\mu \chi^\dagger U + U^\dagger D_\mu \chi \rangle \langle D^\mu \chi^\dagger U + U^\dagger D^\mu \chi \rangle \\
& +c_4 \langle D_\mu U^\dagger \chi - \chi^\dagger D_\mu U \rangle \langle D^\mu U^\dagger \chi - \chi^\dagger D^\mu U \rangle \\
& +c_5 \langle D_\mu \chi^\dagger U - U^\dagger D_\mu \chi \rangle \langle D^\mu \chi^\dagger U - U^\dagger D^\mu \chi \rangle + h_{(2,2)} \langle D_\mu \chi^\dagger D^\mu \chi \rangle \}. \quad (2.14)
\end{aligned}$$

$$\begin{aligned}
\mathcal{L}_{(0,4)} = & \frac{1}{4} F^2 \left\{ e_1 \langle (\chi^\dagger U)^4 + (U^\dagger \chi)^4 \rangle + e_2 \langle \chi^\dagger \chi (\chi^\dagger U \chi^\dagger U + U^\dagger \chi U^\dagger \chi) \rangle \right. \\
& + e_3 \langle \chi^\dagger \chi U^\dagger \chi \chi^\dagger U \rangle + f_1 \langle (\chi^\dagger U)^2 + (U^\dagger \chi)^2 \rangle^2 \\
& + f_2 \langle (\chi^\dagger U)^3 + (U^\dagger \chi)^3 \rangle \langle \chi^\dagger U + U^\dagger \chi \rangle + f_3 \langle \chi^\dagger \chi (\chi^\dagger U + U^\dagger \chi) \rangle \langle \chi^\dagger U + U^\dagger \chi \rangle \\
& + f_4 \langle (\chi^\dagger U)^2 + (U^\dagger \chi)^2 \rangle \langle \chi^\dagger U + U^\dagger \chi \rangle^2 + f_5 \langle (\chi^\dagger U)^3 - (U^\dagger \chi)^3 \rangle \langle \chi^\dagger U - U^\dagger \chi \rangle \\
& + h_4 \langle \chi^\dagger \chi \chi^\dagger \chi \rangle + h_5 \langle \chi^\dagger \chi \rangle (\det \chi + \det \chi^\dagger) \\
& \left. + h_6 (\det \chi + \det \chi^\dagger)^2 + h_7 (\det \chi - \det \chi^\dagger)^2 \right\}. \quad (2.15)
\end{aligned}$$

The lagrangian $\mathcal{L}_{(4,0)}$ is the same as in Ref. [7]. The remaining terms of the $\mathcal{O}(p^4)$ lagrangian of Ref. [7], related to the explicit chiral symmetry breaking sector of the theory, have been redefined; the correspondence reads:

$$A = \frac{2B^2}{F^2}(l_3 + l_4), \quad Z^P = \frac{B^2}{F^2}(-l_3 - l_4 + l_7), \quad \xi^{(2)} = \frac{2B}{F^2}l_4, \quad (2.16)$$

$$h_0 = \frac{4B^2}{F^2}(-l_4 + h_1 + h_3), \quad h'_0 = \frac{4B^2}{F^2}(l_3 + h_1 - h_3). \quad (2.17)$$

The divergences at $\mathcal{O}(p^4)$ in dimensional regularization are absorbed by the following renormalization of the coupling constants⁴

$$\text{const} = \text{const}^r + \Gamma_{\text{const}} \lambda, \quad (2.18)$$

with

$$\lambda = \frac{1}{16\pi^2} \mu^{d-4} \left\{ \frac{1}{d-4} - \frac{1}{2} (\log 4\pi + \Gamma'(1) + 1) \right\}, \quad (2.19)$$

and the Γ_{const} , calculated with the standard heat kernel technique, are collected in the Table 1. We see from the table that, due to the chiral counting of B , the divergences come all at order p^4 , as they should.

⁴A more detailed description of the generating functional, as well as the correspondence between the SU(2) and the SU(3) constants, will be given elsewhere [21].

const	$F^2\Gamma_{\text{const}}$	const	$F^2\Gamma_{\text{const}}$	const	$F^2\Gamma_{\text{const}}$
A	$3B^2$	a_1	$-2Z^P$	e_1	$-2(2A^2 + 10AZ^P + 11Z^{P^2})$
Z^P	$-\frac{3}{2}B^2$	a_2	$-12Z^P$	e_2	$-4(A^2 + 3AZ^P + 4Z^{P^2})$
h_0	0	a_3	0	e_3	$-4(3A^2 + 12AZ^P + 16Z^{P^2})$
h'_0	$6B^2$	b_1	$6(A + Z^P)$	f_1	$3(A^2 + 4AZ^P + 5Z^{P^2})$
$\xi^{(2)}$	$4B$	b_2	$-2(A + Z^P)$	f_2	$2(A^2 + 5AZ^P + 4Z^{P^2})$
$\rho_1^{(2)}$	$-4B(A + Z^P)$	b_3	0	f_3	$4(A^2 + 5AZ^P + 6Z^{P^2})$
$\rho_2^{(2)}$	$-4B(A - 3Z^P)$	c_1	$2(A + 2Z^P)$	f_4	$-6(AZ^P + Z^{P^2})$
$\rho_3^{(2)}$	$2B(A + 3Z^P)$	c_2	0	f_5	$2(A^2 + 5AZ^P + 4Z^{P^2})$
$\rho_4^{(2)}$	$2B(3A + Z^P)$	c_3	0	h_4	$4(A^2 + 2AZ^P + 2Z^{P^2})$
$\rho_5^{(2)}$	$4B(A - 2Z^P)$	c_4	$2A$	h_5	$-4(A^2 + 7AZ^P + 8Z^{P^2})$
l_1	$\frac{1}{3}$	c_5	0	h_6	$2(2A^2 + 4AZ^P + 3Z^{P^2})$
l_2	$\frac{2}{3}$	$h_{(2,2)}$	0	h_7	$-14Z^{P^2}$
l_5	$-\frac{1}{6}$				
l_6	$-\frac{1}{3}$				
h_2	$\frac{1}{12}$				

Table 1: The β function coefficients of the low energy constants. The scale dependence is $\mu(d/d\mu)\text{const}^r = -1/(16\pi^2)\Gamma_{\text{const}}$.

3. Kinematics

There are two different charge modes in the decay $\tau \rightarrow 3\pi\nu_\tau$, the $2\pi^0\pi^-$ mode and the all charged one, $2\pi^-\pi^+$. The relevant hadronic matrix elements are

$$\begin{aligned} H_\mu^{00-}(p_1, p_2, p_3) &= \langle \pi^0(p_1)\pi^0(p_2)\pi^-(p_3) | A_\mu^- | 0 \rangle, \\ H_\mu^{-+-}(p_1, p_2, p_3) &= \langle \pi^-(p_1)\pi^-(p_2)\pi^+(p_3) | A_\mu^- | 0 \rangle, \end{aligned} \quad (3.1)$$

with $A_\mu^- = \bar{u}\gamma_\mu\gamma_5 d$. Both these matrix elements can be simply expressed as follows:

$$H_\mu^{-+-}(p_1, p_2, p_3) = \sqrt{2} [H_\mu^{+-0}(p_3, p_2, p_1) + H_\mu^{+-0}(p_3, p_1, p_2)], \quad (3.2)$$

$$\begin{aligned} H_\mu^{00-}(p_1, p_2, p_3) &= \frac{1}{2} [H_\mu^{--+}(p_2, p_3, p_1) + H_\mu^{--+}(p_1, p_3, p_2) - H_\mu^{--+}(p_1, p_2, p_3)] \\ &= \sqrt{2} H_\mu^{+-0}(p_1, p_2, p_3), \end{aligned} \quad (3.3)$$

with

$$H_\mu^{+-0}(p_1, p_2, p_3) = \langle \pi^+(p_1)\pi^-(p_2)\pi^0(p_3) | A_\mu^0 | 0 \rangle, \quad (3.4)$$

and

$$A_\mu^0 = \bar{u}\gamma_\mu\gamma_5 u - \bar{d}\gamma_\mu\gamma_5 d. \quad (3.5)$$

H_μ^{+-0} contains directly as pole the invariant amplitude $A(s|t, u)$ of the elastic $\pi\pi$ scattering. Both Eqs. (3.2)-(3.3) follow from isospin and charge conjugation symmetry. The most general Lorentz structure of the matrix elements compatible with G-parity invariance is

$$H_\mu^{\text{hfs}}(p_1, p_2, p_3) = V_{1\mu} F_1^{\text{hfs}}(p_1, p_2, p_3) + V_{2\mu} F_2^{\text{hfs}}(p_1, p_2, p_3) + V_{4\mu} F_4^{\text{hfs}}(p_1, p_2, p_3), \quad (3.6)$$

where hfs (hadronic final state) stands for 00– or – – + and

$$\begin{aligned} V_1^\mu &= p_1^\mu - p_3^\mu - \frac{Q(p_1 - p_3)}{Q^2} Q^\mu, \\ V_2^\mu &= p_2^\mu - p_3^\mu - \frac{Q(p_2 - p_3)}{Q^2} Q^\mu, \\ V_4^\mu &= p_1^\mu + p_2^\mu + p_3^\mu = Q^\mu. \end{aligned} \quad (3.7)$$

The G-parity violating contribution $i\epsilon^{\mu,\alpha,\beta,\gamma} p_{1\alpha} p_{2\beta} p_{3\gamma} F_3(p_1, p_2, p_3)$ would be present if $m_u \neq m_d$. However, such a term could only originate from the WZW anomaly, which does not depend on quark masses. Therefore it will start to contribute only at the loop level, that is, in the case of the anomaly, at order $\mathcal{O}(p^6)$. Notice that, in general, $m_u - m_d$ corrections are expected to be of smaller relative importance in the case of small condensate, since the ratio $(m_u - m_d) / (m_u + m_d)$ should decrease. For both the $2\pi^-\pi^+$ and $2\pi^0\pi^-$ final states, Bose symmetry requires

$$F_2^{\text{hfs}}(p_1, p_2, p_3) = F_1^{\text{hfs}}(p_2, p_1, p_3). \quad (3.8)$$

F_1 (F_2) and F_4 correspond respectively to a final hadronic state of total spin 1 and 0, as it is easily seen in the hadronic rest frame. The differential decay rate is given by

$$d\Gamma(\tau \rightarrow 3\pi\nu_\tau) = \frac{(2\pi)^4}{2M_\tau} |\mathcal{M}|^2 d\Phi_4. \quad (3.9)$$

\mathcal{M} is the matrix element of the electroweak interaction

$$\mathcal{M} = V_{\text{ud}} \frac{G_F}{\sqrt{2}} L^\mu H_\mu^{\text{hfs}}, \quad (3.10)$$

with

$$L_\mu = \bar{u}_{\nu_\tau}(p_{\nu_\tau}, s_{\nu_\tau}) \gamma_\mu \gamma_5 u_\tau(p_\tau, s_\tau), \quad (3.11)$$

and $d\Phi_4$ is the invariant phase space of four particles

$$d\Phi_4 = \frac{1}{256} \frac{d\Omega_h}{(2\pi)^{12}} \frac{M_\tau^2 - Q^2}{M_\tau^2} \frac{dQ^2}{Q^2} d\alpha d\gamma d\cos\beta ds_1 ds_2. \quad (3.12)$$

$d\Omega_h$ is the solid angle element of the hadronic system in the τ rest frame and can be written, after integration over the azimuthal direction, as

$$d\Omega_h = 2\pi (d\cos\theta), \quad (3.13)$$

where θ is then the angle between the laboratory and the hadronic system in the τ rest frame. α , β and γ are the Euler angles which describe the orientation of the hadronic system in the laboratory frame (for detailed definitions see Ref. [19], which we follow closely). The hadronic invariant variables are

$$s_1 = (p_2 + p_3)^2, \quad s_2 = (p_1 + p_3)^2, \quad s_3 = (p_1 + p_2)^2, \quad (3.14)$$

with $s_1 + s_2 + s_3 = Q^2 + 3M_\pi^2$.

As shown by Kuhn and Mirkes [19], the matrix element squared can be written in terms of 9 independent leptonic and hadronic real structure functions L_X and W_X

$$|\mathcal{M}|^2 = V_{\text{ud}}^2 \frac{G_F^2}{2} \sum_X L_X W_X. \quad (3.15)$$

All the angular dependence is contained in the functions L_X 's while the W_X 's only depend on the hadronic invariant mass Q^2 and on the Dalitz plot variables s_1 and s_2 . Four of the hadronic structure functions correspond to the square of the spin 1 part of the hadronic matrix element,

$$\begin{aligned} W_A &= (x_1^2 + x_3^2)|F_1|^2 + (x_2^2 + x_3^2)|F_2|^2 + 2(x_1x_2 - x_3^2)\text{Re}(F_1F_2^*), \\ W_C &= (x_1^2 - x_3^2)|F_1|^2 + (x_2^2 - x_3^2)|F_2|^2 + 2(x_1x_2 + x_3^2)\text{Re}(F_1F_2^*), \\ W_D &= 2[x_1x_3|F_1|^2 - x_2x_3|F_2|^2 + x_3(x_2 - x_1)\text{Re}(F_1F_2^*)], \\ W_E &= -2x_3(x_1 + x_2)\text{Im}(F_1F_2^*), \end{aligned} \quad (3.16)$$

one is the square of the spin 0 component

$$W_{SA} = Q^2|F_4|^2, \quad (3.17)$$

and the remaining ones are the interference between the spin 0 and spin 1 components

$$\begin{aligned} W_{SB} &= 2\sqrt{Q^2}[x_1\text{Re}(F_1F_4^*) + x_2\text{Re}(F_2F_4^*)], \\ W_{SC} &= -2\sqrt{Q^2}[x_1\text{Im}(F_1F_4^*) + x_2\text{Im}(F_2F_4^*)], \\ W_{SD} &= 2\sqrt{Q^2}x_3[\text{Re}(F_1F_4^*) - \text{Re}(F_2F_4^*)], \\ W_{SE} &= -2\sqrt{Q^2}x_3[\text{Im}(F_1F_4^*) - \text{Im}(F_2F_4^*)]. \end{aligned} \quad (3.18)$$

The x_i are kinematical functions which are linear in the pion three-momenta in the hadronic rest frame⁵, $x_1 = V_1^x$, $x_2 = V_2^x$ and $x_3 = V_1^y$: they vanish at the production threshold and can be expressed as follows:

$$\begin{aligned} x_1x_2 - x_3^2 &= (Q^2/2 - s_3 - M_\pi^2/2) + (s_3 - s_1)(s_3 - s_2)/(4Q^2), \\ x_1 + x_2 &= -3/2\sqrt{h_0}, \\ x_3 &= \sqrt{h}, \\ -h_0 &= 4M_\pi^2 - (2M_\pi^2 - s_1 - s_2)^2/Q^2, \\ h &= [s_1s_2s_3 - M_\pi^2(Q^2 - M_\pi^2)^2]/(h_0Q^2). \end{aligned} \quad (3.19)$$

⁵This system is oriented in such a way that the x -axis is along the direction of \vec{p}_3 and all the pion fly in the x - y plane.

We can see, from the explicit expressions for the W_X 's, that the purely spin 1 structure functions are suppressed, at threshold, by two powers of the x_i 's, the interferences of spin 1 and spin 0 by one power whereas the purely spin 0 structure function is not suppressed at all. This fact, as already pointed out in the introduction, allows us to have, at threshold, a much larger sensitivity to the S-wave, and then to the size of chiral symmetry breaking measured by the divergence of the axial current.

4. The hadronic matrix element in $G_\chi\text{PT}$

We have seen how the hadronic matrix elements for both the charge modes can be expressed in terms of $H^{+-0}(p_1, p_2, p_3)$. It is then sufficient to compute this quantity: from the residue of the pion pole we will immediately read the $\pi\pi$ scattering amplitude. The $G_\chi\text{PT}$ result at one loop level is

$$\begin{aligned}
iH_\mu^{+-0}(p_1, p_2, p_3) = & \frac{-F_\pi Q_\mu}{Q^2 - M_\pi^2} A(s_3|s_1, s_2) \\
& + \frac{Q_\mu}{F_\pi} \left\{ 1 + \xi^{(2)r} \hat{m} - 2(\xi^{(2)} \hat{m})^2 + (4a_2^r + 4a_3 + 4b_1^r + 4b_2^r + 8c_1^r - 4c_2) \hat{m}^2 \right. \\
& + 2 \frac{l_1^r}{F_\pi^2} (s_3 - 2M_\pi^2) - \frac{l_6^r}{F_\pi^2} (s_1 + s_2 - 2M_\pi^2) + \frac{1}{F_\pi^2} \left(\frac{1}{2} s_3 + 8A \hat{m}^2 \right) J^r(s_3) \\
& + \frac{1}{F_\pi^2} [s_1 M^r(s_1) + s_2 M^r(s_2)] \\
& - \frac{1}{32\pi^2 F_\pi^2} \left[-\frac{1}{3} M_\pi^2 + 8A \hat{m}^2 + \frac{1}{6} (s_1 + s_2) - \frac{1}{9} Q^2 \right] \\
& - \frac{1}{32\pi^2 F_\pi^2} \left[-M_\pi^2 + 8A \hat{m}^2 + \frac{1}{2} (s_1 + s_2) - \frac{1}{3} Q^2 \right] \log \frac{M_\pi^2}{\mu^2} \Big\} \\
& - 2 \frac{p_{3\mu}}{F_\pi} \left[1 + \xi^{(2)r} \hat{m} - 2(\xi^{(2)} \hat{m})^2 + (3a_2^r + 4a_3 + 4b_1^r + 2b_2^r + 4c_1^r - 2c_2) \hat{m}^2 \right. \\
& + \frac{2l_1^r}{F_\pi^2} (s_3 - 2M_\pi^2) - \frac{l_2^r}{2F_\pi^2} (s_1 + s_2 - 4M_\pi^2) - \frac{l_6^r}{F_\pi^2} Q^2 - 2 \frac{M_\pi^2}{F_\pi^2} k_{\pi\pi} + \frac{1}{192\pi^2 F_\pi^2} (s_1 + s_2) \\
& + \frac{1}{F_\pi^2} \left(\frac{s_3}{2} + 8A \hat{m}^2 \right) J^r(s_3) + \frac{1}{F_\pi^2} \left(-\frac{1}{4} M_\pi^2 + A \hat{m}^2 \right) (J^r(s_1) + J^r(s_2)) \Big] \\
& + \frac{1}{F_\pi^3} (p_1 - p_2)_\mu \left[l_2^r (s_2 - s_1) + \left(\frac{1}{3} s_2 - \frac{5}{6} M_\pi^2 - 2A \hat{m}^2 \right) J^r(s_2) \right. \\
& \left. - \left(\frac{1}{3} s_1 - \frac{5}{6} M_\pi^2 - 2A \hat{m}^2 \right) J^r(s_1) + \frac{1}{288\pi^2} (s_2 - s_1) \right]. \tag{4.1}
\end{aligned}$$

The scale dependence of the l.e.c.'s is absorbed by the corresponding dependence in the standard loop functions $J^r(s)$ and $M^r(s)$, defined *e.g.* in Ref. [8], and in the chiral logarithm

$$k_{\pi\pi} = \frac{1}{32\pi^2} \left(\log \frac{M_\pi^2}{\mu^2} + 1 \right), \tag{4.2}$$

so that the total result is independent of the χ PT scale. $A(s_3|s_1, s_2)$ is the (scale independent) off shell $\pi\pi$ scattering amplitude, with $s_1 + s_2 + s_3 = 3M_\pi^2 + Q^2$,

$$\begin{aligned}
A(s_3|s_1, s_2) = & \frac{\beta}{F_\pi^2} \left(s_3 - \frac{4}{3} M_\pi^2 \right) + \alpha \frac{M_\pi^2}{3F_\pi^2} \\
& + \frac{1}{48\pi^2 F_\pi^4} \left(\bar{l}_1 - \frac{4}{3} \right) (s_3 - 2M_\pi^2)^2 \\
& + \frac{1}{48\pi^2 F_\pi^4} \left(\bar{l}_2 - \frac{5}{6} \right) \left[(s_1 - 2M_\pi^2)^2 + (s_2 - 2M_\pi^2)^2 \right] \\
& + \frac{1}{F_\pi^4} \left\{ \frac{1}{2} \left[s_3^2 - M_\pi^4 + 32A\hat{m}^2 s_3 - 24A\hat{m}^2 M_\pi^2 + 112A^2\hat{m}^4 \right] \bar{J}(s_3) \right. \\
& + \left[\left(M_\pi^2 + 4A\hat{m}^2 - \frac{1}{2}s_1 \right)^2 + \frac{1}{12}(s_3 - s_2)(s_1 - 4M_\pi^2) \right] \bar{J}(s_1) \\
& \left. + \left[\left(M_\pi^2 + 4A\hat{m}^2 - \frac{1}{2}s_2 \right)^2 + \frac{1}{12}(s_3 - s_1)(s_2 - 4M_\pi^2) \right] \bar{J}(s_2) \right\}, \quad (4.3)
\end{aligned}$$

Putting $Q^2 = M_\pi^2$ one recovers the $\pi\pi$ amplitude written in the same form as in Ref. [11] (dropping $\mathcal{O}(p^6)$ contributions). The expressions of the scale-independent parameters α , β , \bar{l}_1 and \bar{l}_2 in terms of the low energy constants are given by the following equations:

$$\begin{aligned}
\frac{F_\pi^2}{F^2} M_\pi^2 = & 2B\hat{m} + 4A^r \hat{m}^2 + (9\rho_1^r + \rho_2^r + 20\rho_4^r + 2\rho_5^r) \hat{m}^3 \\
& + (16e_1^r + 4e_2^r + 32f_1^r + 40f_2^r + 8f_3^r + 96f_4^r) \hat{m}^4 \\
& + 4a_3 M_\pi^2 \hat{m}^2 - \frac{M_\pi^2}{32\pi^2 F_\pi^2} (3M_\pi^2 + 20A\hat{m}^2) \log \frac{M_\pi^2}{\mu^2}, \quad (4.4)
\end{aligned}$$

$$\begin{aligned}
F_\pi^2 = & F^2 \left[1 + 2\xi^{(2),r} \hat{m} + (2a_1^r + a_2^r + 4a_3 + 2b_1^r - 2b_2^r) \hat{m}^2 \right. \\
& \left. - \frac{M_\pi^2}{8\pi^2 F_\pi^2} \log \frac{M_\pi^2}{\mu^2} \right], \quad (4.5)
\end{aligned}$$

$$\begin{aligned}
\beta = & 1 + 2\xi^{(2),r} \hat{m} - 4\xi^{(2),r} \hat{m}^2 + 2(3a_2^r + 2a_3 + 4b_1^r + 2b_2^r + 4c_1^r) \hat{m}^2 \\
& - \frac{4M_\pi^2}{32\pi^2 F_\pi^2} \left(1 + 10 \frac{A\hat{m}^2}{M_\pi^2} \right) \left(\log \frac{M_\pi^2}{\mu^2} + 1 \right), \quad (4.6)
\end{aligned}$$

$$\begin{aligned}
\alpha M_\pi^2 \frac{F_\pi^2}{F^2} = & 2B\hat{m} + 16A^r \hat{m}^2 - 4M_\pi^2 \xi^{(2),r} \hat{m} \\
& + (81\rho_1^r + \rho_2^r + 164\rho_4^r + 2\rho_5^r) \hat{m}^3 \\
& - 8M_\pi^2 (2b_1^r - 2b_2^r - a_3 - 4c_1^r) \hat{m}^2 \\
& + 16(6Aa_3 + 16e_1^r + e_2^r + 32f_1^r + 34f_2^r + 2f_3^r + 72f_4^r) \hat{m}^4 \\
& - \frac{M_\pi^2}{32\pi^2 F_\pi^2} \left(4M_\pi^2 + 204A\hat{m}^2 + 528 \frac{A^2\hat{m}^4}{M_\pi^2} \right) \log \frac{M_\pi^2}{\mu^2} \\
& - \frac{1}{32\pi^2 F_\pi^2} \left[M_\pi^4 + 88A\hat{m}^2 M_\pi^2 + 528A^2\hat{m}^4 \right], \quad (4.7)
\end{aligned}$$

$$\bar{l}_1 = 96\pi^2 l_1^r(\mu) - \log \frac{M_\pi^2}{\mu^2}, \quad (4.8)$$

$$\bar{l}_2 = 48\pi^2 l_2^r(\mu) - \log \frac{M_\pi^2}{\mu^2}. \quad (4.9)$$

The parameter α contains the main information about the size of the quark condensate: at tree level it varies between 1 and 4 if $\langle \bar{q}q \rangle$ decreases from its standard value down to zero⁶, while β stays always close to 1. Solving Eq. (4.7) for A and Eq. (4.6) for $\xi^{(2)}$, we can express the form factors in terms of α and β . The result for the $2\pi^0\pi^-$ mode in terms of the form factors $F_1(p_1, p_2, p_3)$ and $F_4(p_1, p_2, p_3)$ introduced in Section 3 is:

$$\begin{aligned} \frac{F_\pi}{\sqrt{2}} F_1^{00-} = & \frac{1}{3}(\beta + 1) + \frac{4}{3}(a_3 - c_2)\hat{m}^2 + \frac{1}{96\pi^2 F_\pi^2} \left[-4M_\pi^2 - 2Q^2 + \frac{2}{3}s_2 + 4s_1 \right. \\ & + \frac{4}{3}\bar{l}_1(s_3 - 2M_\pi^2) + \frac{4}{3}\bar{l}_2(2M_\pi^2 + s_2 - 2s_1) + \frac{2}{3}\bar{l}_6 Q^2 \Big] \\ & + \frac{1}{3F_\pi^2} \left[s_3 + \frac{4}{3}M_\pi^2(\alpha - 1) \right] \bar{J}(s_3) + \frac{1}{3F_\pi^2} \left[s_2 - \frac{2}{3}M_\pi^2\left(\frac{\alpha}{2} + 4\right) \right] \bar{J}(s_2) \\ & + \frac{1}{3F_\pi^2} \left[-s_1 + \frac{2}{3}M_\pi^2(\alpha + 2) \right] \bar{J}(s_1), \end{aligned} \quad (4.10)$$

$$\begin{aligned} \frac{F_\pi}{\sqrt{2}} F_4^{00-} = & \frac{s_3 - M_\pi^2}{2Q^2}(\beta + 1) - \frac{1}{Q^2 - M_\pi^2} \left[\beta \left(s_3 - \frac{4}{3}M_\pi^2 \right) + \frac{\alpha}{3}M_\pi^2 \right] \\ & + \left[a_2^r + 2a_3 + 2b_2^r + 4c_1^r - 4c_2 - 2\frac{s_2 + s_1 - 2M_\pi^2}{Q^2}(a_3 - c_2) \right] \hat{m}^2 \\ & - \frac{M_\pi^2}{96\pi^2 F_\pi^2}(\alpha - 1) \log \frac{M_\pi^2}{\mu^2} \\ & + \frac{1}{96\pi^2 F_\pi^2} \left\{ M_\pi^2 \left[6\frac{s_2 + s_1 - 2M_\pi^2}{Q^2} - \alpha - 1 \right] + 3(s_2 + s_1 - 2M_\pi^2) \right. \\ & - \frac{8}{3}Q^2 + \frac{7}{6}\frac{s_2 + s_1}{Q^2}(2Q^2 - 3s_2 - 3s_1 + 6M_\pi^2) - \frac{5}{6}\frac{(s_2 - s_1)^2}{Q^2} \\ & + 2\bar{l}_1\frac{Q^2 - s_2 - s_1 + 2M_\pi^2}{Q^2}(s_3 - 2M_\pi^2) \\ & \left. + \bar{l}_2\frac{1}{Q^2} \left[(s_2 - s_1)^2 + (s_2 + s_1 - 2M_\pi^2)(s_2 + s_1 - 4M_\pi^2) \right] \right\} \\ & + \frac{1}{12F_\pi^2} \left\{ s_2 - 4M_\pi^2 + \frac{s_2 + s_1 - 2M_\pi^2}{Q^2}M_\pi^2(4 - \alpha) \right. \\ & + \frac{s_2 - s_1}{Q^2} \left[2s_2 - M_\pi^2(4 + \alpha) \right] \\ & \left. - \frac{1}{Q^2 - M_\pi^2} \left[3 \left(s_2 - \frac{2}{3}(\alpha + 2)M_\pi^2 \right)^2 + (s_3 - s_1)(s_2 - 4M_\pi^2) \right] \right\} \bar{J}(s_2) \end{aligned}$$

⁶The relation between $\langle \bar{q}q \rangle$ and α at one-loop level will be revisited in another publication [22].

$$\begin{aligned}
& + \frac{1}{12F_\pi^2} \left\{ s_1 - 4M_\pi^2 + \frac{s_2 + s_1 - 2M_\pi^2}{Q^2} M_\pi^2 (4 - \alpha) \right. \\
& + \frac{s_1 - s_2}{Q^2} [2s_1 - M_\pi^2 (4 + \alpha)] \\
& - \frac{1}{Q^2 - M_\pi^2} \left[3 \left(s_1 - \frac{2}{3}(\alpha + 2)M_\pi^2 \right)^2 + (s_3 - s_2)(s_1 - 4M_\pi^2) \right] \Big\} \bar{J}(s_1) \\
& + \frac{1}{2F_\pi^2} \left\{ \frac{1}{Q^2} (Q^2 - s_2 - s_1 + 2M_\pi^2) \left[s_3 + \frac{4}{3}M_\pi^2(\alpha - 1) \right] \right. \\
& - \frac{1}{Q^2 - M_\pi^2} \left[s_3^2 + \frac{8}{3}M_\pi^2(\alpha - 1)s_3 + M_\pi^4 \left(\frac{7}{9}\alpha^2 - \frac{32}{9}\alpha + \frac{16}{9} \right) \right] \Big\} \bar{J}(s_3) \\
& - \frac{F_\pi^2}{Q^2 - M_\pi^2} \left\{ \frac{1}{48\pi^2 F_\pi^4} \left(\bar{l}_1 - \frac{4}{3} \right) (s_3 - 2M_\pi^2)^2 \right. \\
& + \frac{1}{48\pi^2 F_\pi^4} \left(\bar{l}_2 - \frac{5}{6} \right) [(s_2 - 2M_\pi^2)^2 + (s_1 - 2M_\pi^2)^2] \Big\}, \tag{4.11}
\end{aligned}$$

where we have defined the scale independent quantities

$$\bar{l}_i = \frac{32\pi^2}{\gamma_i} l_i^r(\mu) - \log \frac{M_\pi^2}{\mu^2}, \tag{4.12}$$

and γ_i are the corresponding β function coefficients collected in Table 1. It is easy to verify, taking the S χ PT expressions for α and β ,

$$\alpha^{\text{st}} = 1 + \left[-\frac{1}{32\pi^2} \left(\log \frac{M_\pi^2}{\mu^2} + 1 \right) + 6l_3^r + 2l_4^r \right] \frac{M_\pi^2}{F_\pi^2}, \tag{4.13}$$

$$\beta^{\text{st}} = 1 + \left[-\frac{1}{8\pi^2} \left(\log \frac{M_\pi^2}{\mu^2} + 1 \right) + 2l_4^r \right] \frac{M_\pi^2}{F_\pi^2}. \tag{4.14}$$

that one recovers the results of Ref. [17]. Notice that the form factor F_4 is proportional to the matrix element of the divergence of the axial current. One easily verifies that the expression (4.11) goes to zero in the chiral limit. These two facts, together with the global renormalization scale independence, provides non-trivial checks of our calculation. It is remarkable that in Eqs. (4.10) and (4.11) all the contributions from the $\tilde{\mathcal{L}}^{(3)}$ lagrangian are absorbed in the definitions of α , β , F_π and M_π .

5. Connection with low-energy $\pi\pi$ observables

The renormalization-group invariant parameters α and β are essentially the (on shell) $\pi\pi$ amplitude $A(s|t, u)$ and its slope at the symmetrical point $s = t = u = 4/3M_\pi^2$. For this reason one expects both α and β to be less sensitive to the higher order chiral corrections than, say, the S-wave scattering lengths. They represent the $\mathcal{O}(p^4)$ G χ PT truncation of observable quantities α and β defined, including $\mathcal{O}(p^6)$ accuracy,

in Ref. [11],

$$A(s|t, u) = A_{\text{KMSF}}(s|t, u; \alpha, \beta; \lambda_1, \lambda_2, \lambda_3, \lambda_4) + \mathcal{O}\left[\left(\frac{p}{\Lambda_H}\right)^8, \left(\frac{M_\pi}{\Lambda_H}\right)^8\right], \quad (5.1)$$

where the function A_{KMSF} is explicitly displayed. Both α and β will be measured in forthcoming high-precision low-energy $\pi\pi$ experiments (Dirac at CERN, E865 at BNL, KLOE at DaΦne). The values of α and β are constrained by the behavior of the phase δ_1^1 in the ρ region, using the Roy dispersion relations [23] (resulting in the so-called Morgan-Shaw universal curve [24]). The parameters $\lambda_1, \dots, \lambda_4$ have been determined in Ref. [25] from medium-energy experimental $\pi\pi$ phases, using a set of rapidly converging sum rules derived from Roy dispersion relations. The results depend very little on the size of $\langle \bar{q}q \rangle$. Comparing the expression (5.1) with the explicit two-loop calculation performed in $\text{S}\chi\text{PT}$ [26] one finds the relationship between the parameters λ_i 's and the low energy constants of the Standard lagrangian [27],

$$\lambda_i = \lambda_i(\bar{l}_1, \bar{l}_2, \bar{l}_4, \dots), \quad i = 1, \dots, 4. \quad (5.2)$$

Notice that the parameters (5.2) do not depend at all on the critical standard $\mathcal{O}(p^4)$ constant \bar{l}_3 , which controls the size of $\langle \bar{q}q \rangle$, and the dependence on the constant \bar{l}_4 shows up only at $\mathcal{O}(p^6)$ order. For this reason Eq. (5.2) can be inverted for \bar{l}_1 and \bar{l}_2 , yielding the values [27]

$$\bar{l}_1 = -0.37 \pm 1.96, \quad \bar{l}_2 = 4.17 \pm 0.47. \quad (5.3)$$

where the error bars come from the uncertainty on the parameters λ_i 's and the estimated uncertainty of higher chiral orders. Strictly speaking the values of Eq. (5.3) have been obtained within the framework of $\text{S}\chi\text{PT}$. However, for the reason mentioned above, the $\mathcal{L}_{(4,0)}$ constants \bar{l}_1 and \bar{l}_2 should not be affected by the variation of the quark condensate. Improvements in the precision of the determination of l_1 and l_2 are expected from forthcoming numerical solutions of Roy Equations [28].

Using the currently available data on $\delta_0^0 - \delta_1^1$ extracted from the last K_{e4}^+ experiment (Rosset et al. [29]) the best fitted values for α and β are [11]:

$$\alpha^{\text{exp}} = 2.16 \pm 0.86, \quad \beta^{\text{exp}} = 1.074 \pm 0.053, \quad (5.4)$$

where the error bars are merely experimental. They have to be compared with the $\text{S}\chi\text{PT}$ $\mathcal{O}(p^4)$ expressions (4.13)-(4.14), which, using for l_3 and l_4 the central values quoted in Ref. [26]

$$l_3^r(M_\rho) = 0.82 \times 10^{-3}, \quad l_4^r(M_\rho) = 5.6 \times 10^{-3}, \quad (5.5)$$

give

$$\alpha^{\text{st}} = 1.06, \quad \beta^{\text{st}} = 1.095. \quad (5.6)$$

Taking further into account the higher order contributions, estimated in Ref. [27], the standard values for α and β become⁷

$$\alpha^{\text{st}} = 1.07 \pm 0.01, \quad \beta^{\text{st}} = 1.105 \pm 0.015. \quad (5.7)$$

Our strategy to detect the sensitivity to the size of $\langle \bar{q}q \rangle$, cross-checking the future determinations from $\pi\pi$ scattering, will be to plot the structure functions for three sets of values of α and β ,

$$\begin{aligned} \alpha^{\text{st}} &= 1.07, & \beta^{\text{st}} &= 1.105, \\ \alpha^{\text{exp}} &= 2.16, & \beta^{\text{exp}} &= 1.074, \\ \alpha &= 4, & \beta &= 1.16. \end{aligned} \quad (5.8)$$

They correspond respectively to the S χ PT predictions, Eq. (5.7), the central values obtained from the best fit to the Rosselet *et al.* data [29], Eq. (5.4) and the extreme case of tiny condensate ($\alpha = 4$ with the corresponding $\beta = 1.16$ inferred from the Morgan-Show universal curve).

The other numerical input for the form factors (not entering the $\pi\pi$ amplitude) that we will use is the value of \bar{l}_6 , from the two-loop analysis of the vector form factor of the pion [30],

$$\bar{l}_6 = 16.0 \pm 0.9. \quad (5.9)$$

The contributions from the low energy constants of $\mathcal{L}_{(2,2)}$ and $\mathcal{L}_{(0,4)}$ will be considered as sources of error, with zero central values and errors according to naïve dimensional analysis estimates, that is

$$c_{(2,2)} = 0 \pm \frac{1}{\Lambda_{\text{H}}^2}, \quad c_{(0,4)} = 0 \pm \frac{1}{\Lambda_{\text{H}}^4}, \quad (5.10)$$

where Λ_{H} is the typical mass of the resonance exchanged, say $\Lambda_{\text{H}} \sim 1$ GeV.

6. Structure functions and azimuthal asymmetries

In this section we will give the numerical results for the structure functions integrated over the whole Dalitz plot, at fixed Q^2 ,

$$\begin{aligned} w_{A,C,SA,SB,SC} &= \int ds_1 ds_2 W_{A,C,SA,SB,SC}(Q^2, s_1, s_2), \\ w_{D,E,SD,SE} &= \int ds_1 ds_2 \text{sign}(s_1 - s_2) W_{D,E,SD,SE}(Q^2, s_1, s_2), \end{aligned} \quad (6.1)$$

⁷Both the values (5.3) and the S χ PT prediction (5.7) are compatible with the central values referred to as “Set II” given in Ref. [13] without error bars. Notice that the errorbars given in Eq. (5.7) do not include any uncertainty due to l_3 and l_4 . Eq. (5.5) is taken as our *definition* of the standard case.

where the sign ordering is needed due to the Bose symmetry. The limits of integration of s_2 for a given value of s_1 are $s_2^- < s_2 < s_2^+$ where

$$s_2^\pm = 2M_\pi^2 + 2E_1E_3 \pm 2\sqrt{E_1^2 - M_\pi^2}\sqrt{E_3^2 - M_\pi^2} \quad (6.2)$$

and

$$E_1 = \frac{Q^2 - M_\pi^2 - s_1}{2\sqrt{s_1}}, \quad E_3 = \frac{1}{2}\sqrt{s_1} \quad (6.3)$$

are the energies of the particles 1 and 3 in the 2-3 rest frame (*i.e.* in the system where $\vec{p}_2 + \vec{p}_3 = 0$), while the bounds of s_1 are

$$4M_\pi^2 < s_1 < \left(\sqrt{Q^2} - M_\pi\right)^2. \quad (6.4)$$

Due to the presence of two identical particles an additional factor 1/2 has to be understood in the integration over the Dalitz plot. The results for both the charge modes are shown in Figs. 1 and 2. In both cases w_A and w_C are practically indistinguishable at the scale of the plots. The reason for that is, as already pointed out in Ref. [17], that

$$W_A - W_C = 2x_3^2|F_1 - F_2|^2, \quad (6.5)$$

where $F_1 - F_2$ is antisymmetric with respect to the exchange of the particles 1 and 2, and, as it is clear from Eq. (4.1), the antisymmetric part starts at order $\mathcal{O}(p^4)$. w_A is the main contribution to the total decay rate:

$$d\Gamma = \frac{G_F^2}{128M_\tau} \frac{V_{ud}^2}{(2\pi)^5} \left[\frac{M_\tau^2 - Q^2}{Q^2} \right]^2 \frac{M_\tau^2 + 2Q^2}{3M_\tau^2} W(Q^2) dQ^2 \quad (6.6)$$

where

$$W(Q^2) = w_A + \frac{3M_\tau^2}{M_\tau^2 + 2Q^2} w_{SA}. \quad (6.7)$$

and we can see that most of the other structure functions are much smaller compared to it. The solid, dashed and dotted lines correspond to the three sets of values of Eq. (5.8) discussed above. We see that all the spin 1 structure functions practically do not depend on $\langle \bar{q}q \rangle$ (except w_D for the all charged mode, which, being zero at the tree level, is very small and very much affected by the theoretical uncertainties). On the contrary a rather strong dependence is observed not only in the purely spin 0, but also in the interference terms w_{SB}, \dots, w_{SE} . In particular, among the latters, w_{SB} is the largest one and its magnitude is comparable to w_A . Clearly, w_{SB} is the most appropriate structure function where to look for the S-wave contribution. From the experimental point of view, the sensitivity to the size of $\langle \bar{q}q \rangle$ should therefore be expected in azimuthal angular asymmetries (see Ref. [32]). These are obtained by integrating the differential decay rate (3.9) over all the variables except Q^2 and the

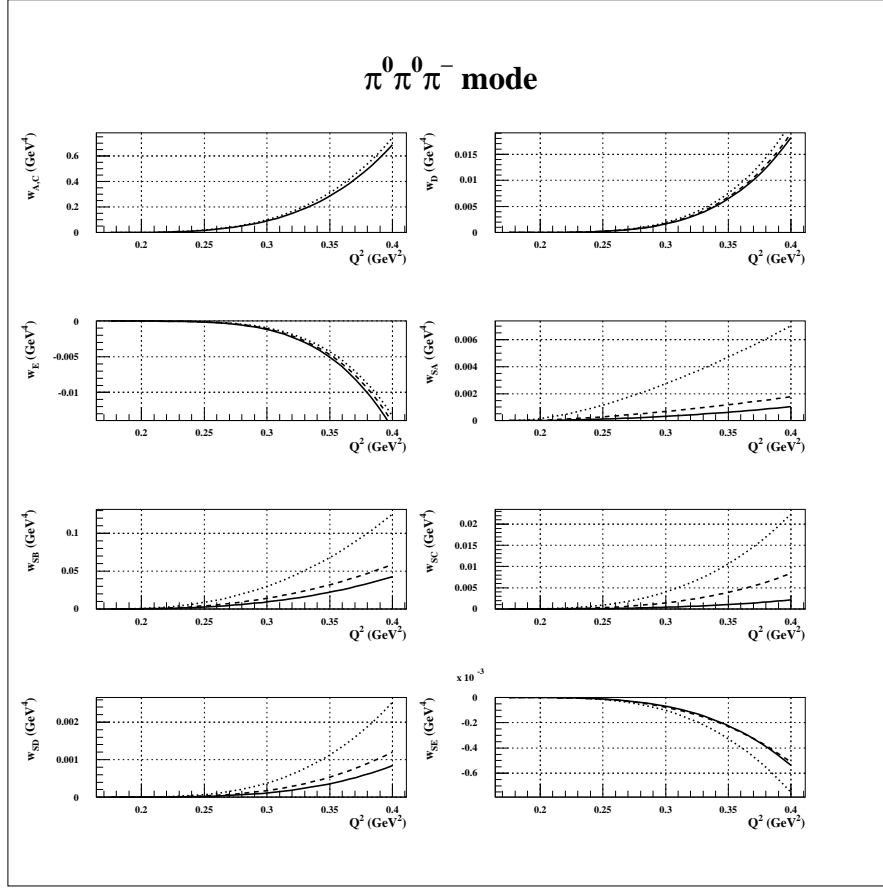


Figure 1: Integrated structure functions for the $\pi^0\pi^0\pi^-$ charge mode. w_A and w_C (here and in the next figure) are indistinguishable at the scale of the plot. Solid, dashed and dotted lines refer to the three sets of values for α and β of Eq. (5.8). They correspond respectively to the standard predictions, the central values extracted from the K_{e4} experiment, and to the extreme case of tiny condensate.

azimuthal angle γ , using the explicit angular dependence of the functions L_X found in Ref. [19]:

$$d\Gamma = \frac{G_F^2}{128M_\tau} \frac{1}{(2\pi)^5} V_{ud}^2 \left[\frac{M_\tau^2 - Q^2}{Q^2} \right]^2 \frac{M_\tau^2 + 2Q^2}{3M_\tau^2} f(Q^2, \gamma) W(Q^2) dQ^2 \frac{d\gamma}{2\pi}, \quad (6.8)$$

with $W(Q^2)$ defined above and the azimuthal distribution, normalized to 1,

$$f(Q^2, \gamma) = 1 + \lambda_2(Q^2, \beta_\tau) (C'_{LR} \cos 2\gamma + C'_{UD} \sin 2\gamma) + \lambda_1(Q^2, \beta_\tau) (C_{LR} \cos \gamma + C_{UD} \sin \gamma). \quad (6.9)$$

The asymmetry coefficients C'_{LR} , C'_{UD} , C_{LR} and C_{UD} in Eq. (6.9) are related to the

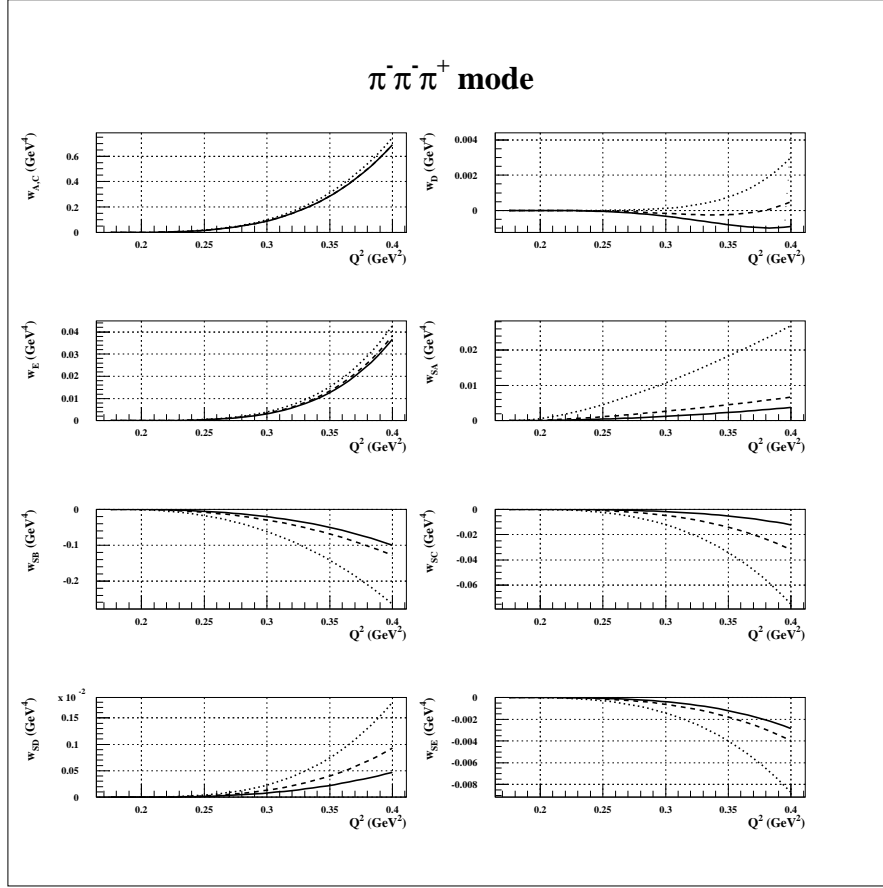


Figure 2: Integrated structure functions for the $2\pi^-\pi^+$ charge mode. The legend is as in the previous figure.

Kuhn and Mirkes' structure functions by the relations⁸

$$\begin{aligned}
 C'_{\text{LR}} &= \frac{1}{3} \left(1 - \frac{Q^2}{M_\tau^2} \right) \frac{3M_\tau^2}{M_\tau^2 + 2Q^2} \frac{w_C}{W}, & C'_{\text{UD}} &= -\frac{1}{3} \left(1 - \frac{Q^2}{M_\tau^2} \right) \frac{3M_\tau^2}{M_\tau^2 + 2Q^2} \frac{w_D}{W}, \\
 C_{\text{LR}} &= -\frac{\pi}{4} \frac{3M_\tau^2}{M_\tau^2 + 2Q^2} \frac{w_{SB}}{W}, & C_{\text{UD}} &= \frac{\pi}{4} \frac{3M_\tau^2}{M_\tau^2 + 2Q^2} \frac{w_{SD}}{W}.
 \end{aligned} \tag{6.10}$$

The interesting quantity is the left-right asymmetry, whose coefficient is related to w_{SB} . The functions λ_i in Eq. (6.9) result from the integration over the τ -decay angle,

$$\lambda_i(Q^2, \beta_\tau) = \int_{-1}^1 \frac{d \cos \theta}{2} P_i(\cos \psi), \tag{6.11}$$

where β_τ is the τ velocity

$$\beta_\tau = \sqrt{1 - \frac{M_\tau^2}{E_{\text{beam}}^2}}, \tag{6.12}$$

⁸We are neglecting the polarization of the τ 's, which is justified provided that the Z exchange can be neglected (far from the Z peak).

and the angle ψ is defined in Ref. [19]. For τ 's produced at rest, which is the case for the τ -charm factories, this angle is $\cos \psi = 1$, so that the functions λ_i are equal to 1, whereas in the ultrarelativistic case, $\beta_\tau = 1$, they become

$$\begin{aligned}\lambda_1(Q^2, 1) &= \frac{1}{(M_\tau^2 - Q^2)^2} \left(M_\tau^4 - Q^4 + 2M_\tau^2 Q^2 \log \frac{Q^2}{M_\tau^2} \right), \\ \lambda_2(Q^2, 1) &= -2 + 3 \frac{M_\tau^2 + Q^2}{M_\tau^2 - Q^2} \lambda_1(Q^2, 1).\end{aligned}\tag{6.13}$$

These two functions are plotted for different values of β_τ in Fig. 3. We see from the

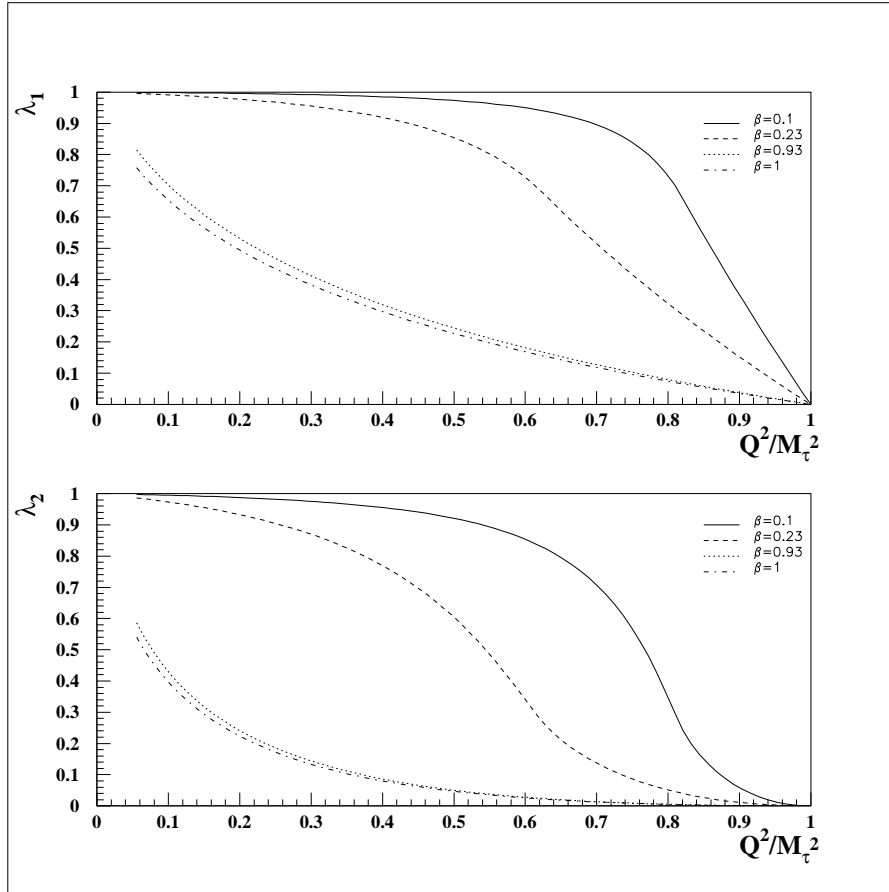


Figure 3: The functions λ_1 and λ_2 for different values of the τ velocity β_τ .

figure that, for high energy machines, the functions λ_i decrease the sensisivity in the threshold region, but the effect is not so drastic, especially for λ_1 , which multiplies the coefficient C_{LR} . In order to take full advantage of the whole statistics we can consider the integrated left-right asymmetry,

$$A_{\text{LR}}(Q^2) = \left| \frac{N_{\text{R}} - N_{\text{L}}}{N_{\text{R}} + N_{\text{L}}} \right| \tag{6.14}$$

where N stands for the number of events from threshold up to a certain Q^2 and the subscript L (R) refers to the events with $\gamma \in [0, \pi/2] \cup [3\pi/2, 2\pi]$ ($\gamma \in [\pi/2, 3\pi/2]$). This asymmetry⁹ for both the charge mode is shown in Fig. 4. The solid lines

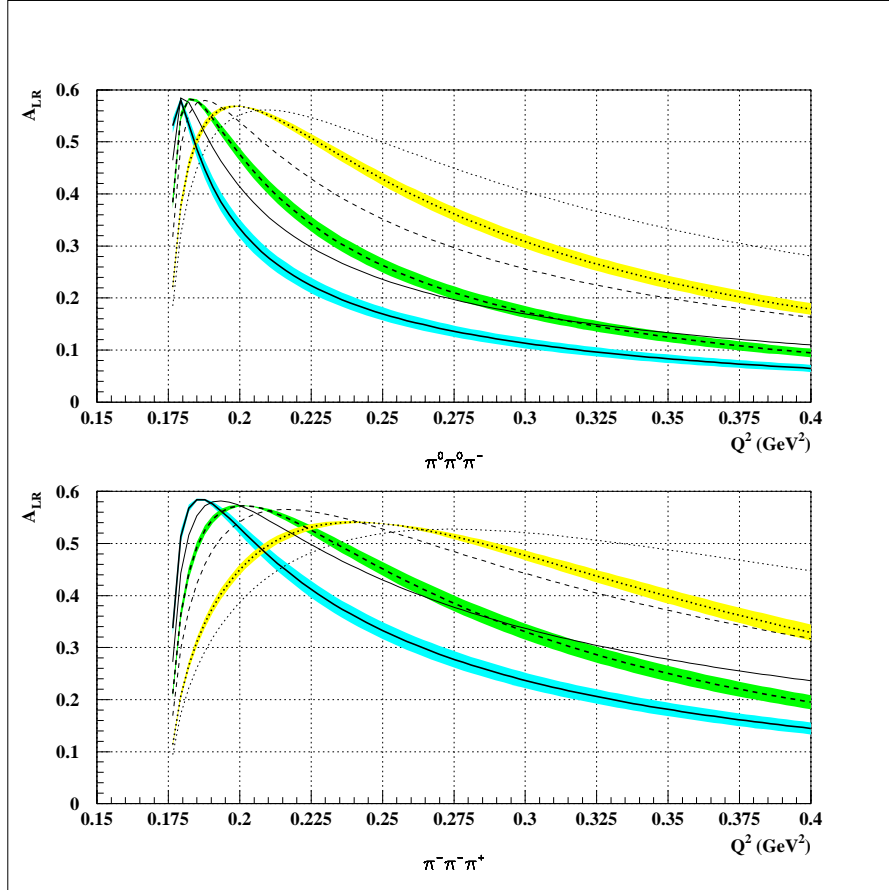


Figure 4: The left right asymmetry, for the two charge modes, as function of Q^2 . The three curves, solid, dashed and dotted, inside the errorband correspond to the three different values of α and β in Eq. (5.8) (like in Figs. 1 and 2). The corresponding lines outside the bands are the results at tree level.

correspond to the standard case, the dashed lines to the central “experimental” values of Eq. (5.4) and the dotted ones to the extreme case of tiny condensate [Eq. (5.8)]. The bands represent the theoretical uncertainties, coming from the errors on the low energy constants [Eqs. (5.3), (5.9) and (5.10)¹⁰] and from a variation of the χ PT renormalization scale μ , at which the estimate (5.10) is supposed to hold, between 500 MeV and 1 GeV. Particular attention has been paid to the sensitivity of the

⁹The results for the asymmetries refer to the case of ultrarelativistic τ ’s, where the asymptotic expressions of Eq. (6.13) can be used.

¹⁰In the estimation of the error from Eq. (5.10) we have taken $\hat{m} \sim 20$ MeV.

structure functions to the two constants \bar{l}_1 and \bar{l}_2 . One sees from Table 2 that for all the asymmetries considered in this paper the uncertainty coming from these two constants is well under control. This would not be the case for the up-down asymmetries, related to the structure functions w_D and w_{SD} . The lines outside

X	A	C	D	E	SA	SB	SC	SD	SE
$\frac{1}{w_X} \frac{\partial w_X^{00-}}{\partial \bar{l}_1}$	0.02	0.02	0.01	0.02	-0.03	-0.004	0.04	-0.02	-0.03
$\frac{1}{w_X} \frac{\partial w_X^{00-}}{\partial \bar{l}_2}$	-0.02	-0.02	0.3	-0.04	-0.06	-0.05	0.009	0.2	-0.2
$\frac{1}{w_X} \frac{\partial w_X^{-+}}{\partial \bar{l}_1}$	0.02	0.02	8	0.005	-0.03	-0.007	0.02	0.6	-0.05
$\frac{1}{w_X} \frac{\partial w_X^{-+}}{\partial \bar{l}_2}$	-0.02	-0.02	8	-0.02	-0.07	-0.05	-0.006	0.6	-0.07

Table 2: The dependence of the nine integrated structure functions w_X on \bar{l}_1 and \bar{l}_2 . The derivatives are computed at $Q^2 = 0.35\text{GeV}^2$.

the bands in Fig. 4 correspond to the result at tree level. We see that the one-loop corrections to the asymmetry are rather important, not exceeding however 30 %. Assuming a geometrical behavior of this series, the two-loop effects are expected to remain in the range of 10 %, which at present stage should be considered as an additional systematic error to the one shown in Figs. 4 and 5. Notice however that a better control of this systematic error is conceivable: *i*) most of this uncertainty comes from the spin 1 part of the matrix element (see also Fig. 6), and consequently an inclusion of the resonance contribution which dominates in this channel might shed more light on the problem; *ii*) the strong final state interaction in the S-wave can be treated more precisely by the standard procedure of unitarization (cfr. Ref. [31]).

In the case of τ leptons produced close to threshold (τ -charm factories), the above asymmetries are somewhat larger since in this case the kinematical functions $\lambda_1 = \lambda_2 = 1$ increase the contribution of the low- Q^2 region to the integrated asymmetries. Taking as reference the value $Q^2 = (600 \text{ MeV})^2$, A_{LR} for the all charged mode goes from $(60 \pm 6)\%$, for tiny condensate ($\alpha = 4$), to $(28 \pm 4)\%$ for the standard case. We emphasize once more that the reason for such a big symmetry breaking effect of the S-wave is the kinematical suppression of the P-wave near the threshold. Another asymmetry where the same argument applies is A'_{LR} , plotted in Fig. 5 (the legend is the same as in the previous figure), which corresponds to the coefficient C'_{LR} . A'_{LR} is defined analogously to Eq. (6.14) with L referring to the events with $\gamma \in [\pi/4, 3\pi/4] \cup [5\pi/4, 7\pi/4]$ and R to the complementary interval. Eventhough this asymmetry is of less practical utility than A_{LR} , it is remarkable that the separation of the three cases near the threshold is entirely due to the purely spin 0 structure function, which is suppressed by two powers of the quark mass. Now that we have the predictions for the azimuthal asymmetries, it is useful to know how many events are expected in the near-threshold region. Using the experimental value of the τ lifetime, χPT is able to predict the integrated branching ratio, that is the

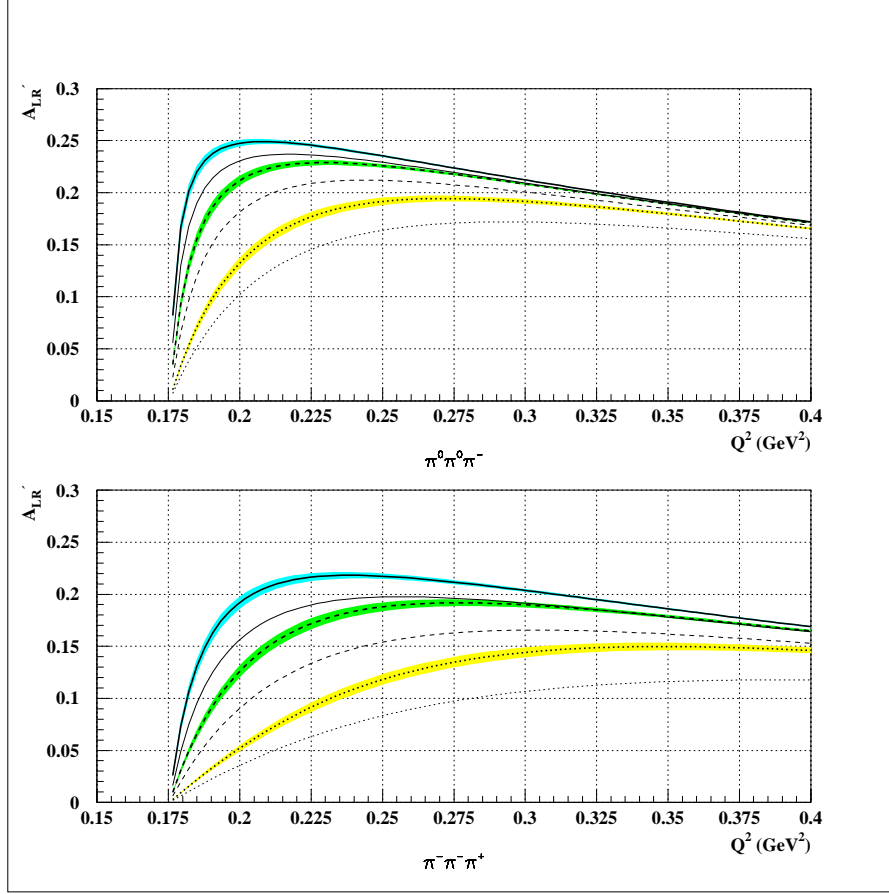


Figure 5: The asymmetry A'_{LR} for the two charge modes, as function of Q^2 . The legend is like in Fig. 4.

number of events from threshold up to a certain Q^2 , divided by the total number of τ produced. This quantity is plotted in Fig. 6. It turns out that it is very similar for both the charge modes. The uncertainties coming from the low energy constants and from a variation of the χ PT renormalization scale between 500 MeV and 1 GeV are invisible at the scale of the plot. On the other hand, we see that the convergence of the χ PT series is much worse than in the case of the asymmetries, as already pointed out (typically the tree level contribution is half of the total one-loop result; cfr. the discussion in Ref. [17]). We thus conclude that, in contrast to the asymmetries, the one-loop χ PT predictions for the branching ratio are less reliable, and should not be used as a basis for a precision test of χ PT. With this in mind, according to Fig. 6, the number of events with $Q^2 < (600 \text{ MeV})^2$ is expected to be of the order of 10^{-5} times the number of τ 's produced. On the experimental side, the largest statistics, up to now, has been collected by CLEO, with a total number of τ pairs of $\sim 10^7$, that is a hundred of events below $(600 \text{ MeV})^2$ for each charge mode of the

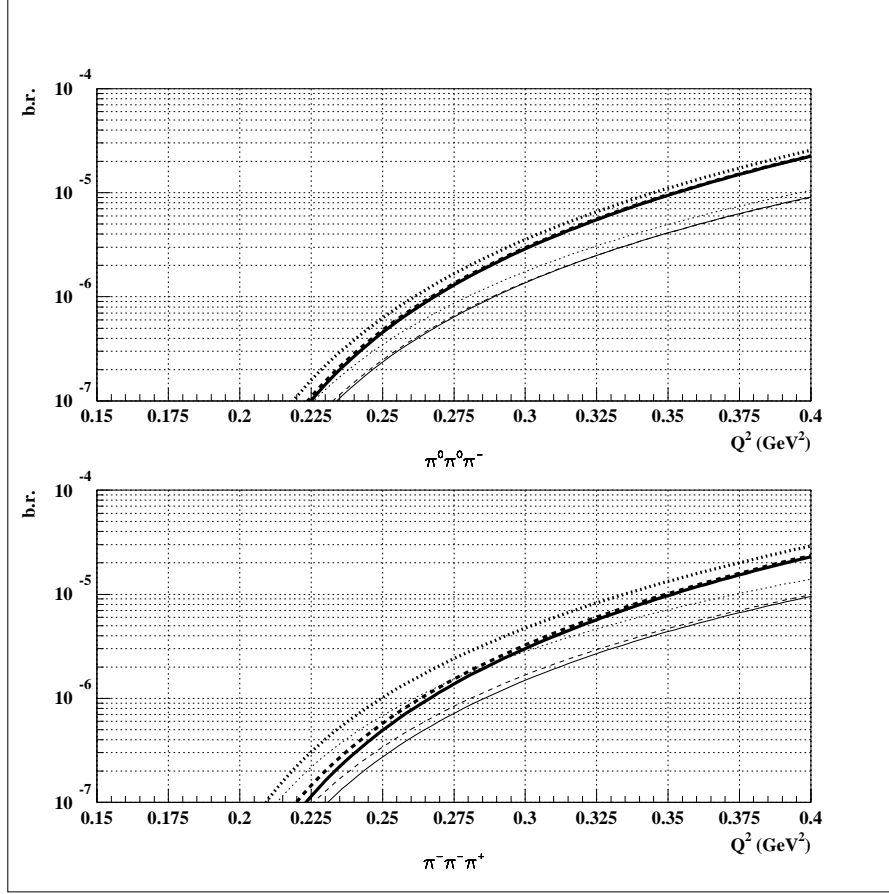


Figure 6: *The integrated branching ratio for the two charge modes. The solid, dashed and dotted lines correspond respectively to the three values of Eq. (5.8) for α and β . The thicker lines are the one loop results and the thinner the corresponding tree level ones.*

decays $\tau \rightarrow 3\pi\nu_\tau$. With such statistics, measuring A_{LR} for the all charged mode, one should already be able to extract α , and then the quark condensate, with a precision comparable to the present one, summarized in Eq. (5.4). According to M. Perl (see Ref. [18]), a factor ~ 5 increase in statistics can reasonably be expected in the near future, thanks to the new high luminosity B -factories. That could allow a much sharper measurement of α , thus providing an interesting and completely independent cross-check of future precise determinations from $\pi\pi$ scattering.

7. The size of the spin 0 spectral function

The scalar structure function $w_{SA}(Q^2)$ is proportional to the three-pion component of the spin 0 τ spectral function, that is the spectral function of the divergence of the axial current. This quantity enters in the sum rule determinations of the light

quark mass \hat{m} . The two-point function relevant for such determinations is

$$\psi_5(Q^2) = i \int d^4x e^{iQ \cdot x} \langle 0 | T \left\{ \partial^\mu (\bar{u} \gamma_\mu \gamma_5 d)(x) \partial^\nu (\bar{d} \gamma_\nu \gamma_5 u)(0) \right\} | 0 \rangle, \quad (7.1)$$

whose imaginary part is proportional to the spectral function

$$\frac{1}{\pi} \text{Im} \psi_5(Q^2) = \rho(Q^2) = \frac{1}{2\pi} \sum_n (2\pi)^4 \delta^4(Q - p_n) \left| \langle n | \partial^\mu (\bar{d} \gamma_\mu \gamma_5 u) | 0 \rangle \right|^2. \quad (7.2)$$

Using the Cauchy's theorem and the analytic properties of the two-point function, one can relate the integral of the spectral function along the positive x -axis, to a contour integral of $\psi_5(Q^2)$ at high energy. Evaluating the latter with the help of perturbative QCD together with the OPE technique for the non perturbative contributions, one arrives to the class of sum rules

$$\int_0^{s_0} dQ^2 Q^{2n} \text{Im} \psi_5(Q^2) = -\frac{1}{2\pi i} \oint_{|Q^2|=s_0} dQ^2 Q^{2n} \psi_5(Q^2). \quad (7.3)$$

The three-pion component of the spin 0 spectral function reads

$$\rho_{3\pi}(Q^2) = \frac{1}{256\pi^4} \left[w_{SA}^{00-}(Q^2) + w_{SA}^{- - +}(Q^2) \right]. \quad (7.4)$$

This is the hadronic phenomenological input that one has to insert, in the low energy part of the l.h.s. of Eq. (7.3) in order to evaluate the sum rule. Due to the smallness of the w_{SA} structure functions, a direct experimental information on $\rho_{3\pi}$ is lacking. Therefore a model for the three-pion continuum has to be used, which should include the observed resonances in this channel. Yet the overall normalization of the spectral function modeled in this way, remains unknown. It has been proposed in Refs. [33, 34] to normalize the hadronic model to the low energy behavior predicted by standard χ PT. However, as we have seen in the previous section, the low energy behavior of w_{SA} depends very much on the size of the quark condensate. In Fig. 7 we plot the ratio

$$R^{(\alpha,\beta)}(Q^2) = \frac{\rho_{3\pi}^{(\alpha,\beta)}(Q^2)}{\rho_{3\pi}^{\text{st}}(Q^2)} \quad (7.5)$$

of the 3-pion component of the spectral function for a given value of α and β divided by the standard χ PT prediction. The two bands correspond to the second and third set of values of Eq. (5.8); also shown are the tree level results. We see that the low energy spectral function increases by a factor of ~ 12 in extreme case of $\alpha = 4$, and the output of the sum rule for \hat{m}^2 can be expected to increase accordingly. In Ref. [32] the threshold behavior of the same ratio has been analyzed neglecting M_π^2 in the integration over the Dalitz plot. The latter approximation is actually not very good near the threshold and overestimates the result: at tree level, in the extreme case of $\alpha = 4$, the ratio $R^{(\alpha,\beta)}(9M_\pi^2)$ was found to be 13.5. However, this effect is compensated by the increase due to the one-loop corrections.

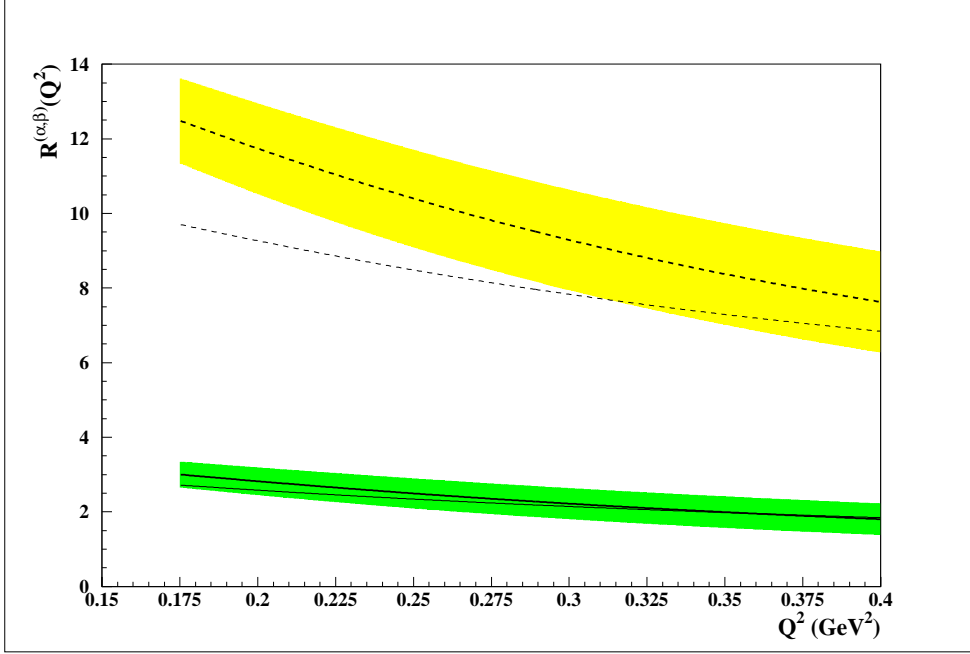


Figure 7: The three-pion component of the spectral function $\rho_{3\pi}(Q^2)$ for $\alpha = 2.16$, $\beta = 1.074$ (solid line) and for $\alpha = 4$, $\beta = 1.16$ (dashed line), normalized to the standard χPT predictions. The lines outside the errorbands are the tree level results.

8. Concluding remarks

The understanding of the mechanism of DBCHS in QCD requires the knowledge of the size of the quark anti-quark condensate. $G\chi PT$ is the appropriate tool to pin down this quantity from low energy experiments. The physical observable that will presumably allow to do that is the low energy $\pi\pi$ scattering. In this paper the $SU(2)\times SU(2)$ generalized chiral lagrangian is constructed to $\mathcal{O}(p^4)$ and renormalized at one-loop level. We have presented an alternative way of extracting $\langle\bar{q}q\rangle$, from the τ decays into three pions, performing an analysis at one-loop level of $G\chi PT$. The dependence on the condensate is contained in the S-wave of these decays, which is an effect of explicit chiral symmetry breaking. However, due to a kinematical suppression of the P-wave, compared to the S-wave, the latter shows up as a detectable effect near the threshold, through the azimuthal left-right asymmetries. At Q^2 large enough to allow for an experimental determination ($Q^2 \sim 0.35\text{GeV}^2$) it turns out that the integrated left-right asymmetry is larger for the all charged mode (see Fig. 4). In the case of ultrarelativistic τ 's (relevant, *e. g.*, for CLEO) the predictions of $G\chi PT$ for this asymmetry, integrated from threshold up to $Q^2 = 0.35\text{GeV}^2$, range from $(17 \pm 2) \%$ (in the standard case) up to $(40 \pm 2) \%$, depending on the size of $\langle\bar{q}q\rangle$. These errorbars do not take into account the uncertainty coming from the

higher chiral orders. We estimate the latter to be $\sim 10\%$ of the total result. Therefore a measurement significantly larger than 20% would already signal a departure from the standard picture of large condensate. Unfortunately the number of events expected in this region is rather small: the branching ratio integrated from threshold to $Q^2 = 0.35\text{GeV}^2$ is of the order of 10^{-5} for each charge mode. The presently available statistics (10^7 $\tau^+\tau^-$ pairs of CLEO) will allow to measure this asymmetry, but not to distinguish between the standard and the extreme generalized case. However improvements can be expected from both theoretical and experimental sides. The theoretical predictions can in principle be sharpened by an analysis “beyond one loop”, which should include, in the spin 1 form factor, the effect of the resonance a_1 (cfr. Ref. [35]) and, in the spin 0 form factor, the strong final state interactions of the S-wave (unitarization procedure [31]). From the experimental point of view an improvement in statistics by a factor $5 \div 10$ seem reachable. That would allow a real measurement of the parameter α , related to $\langle \bar{q}q \rangle$, providing a completely independent cross-check of future precise determinations from $\pi\pi$ scattering.

Acknowledgments

It is a pleasure to thank Marc Knecht for correspondence and discussions. L.G. wishes also to acknowledge useful discussions with Toni Pich. We would like to thank Dominique Vautherin for the hospitality at LPTPE, Université Pierre et Marie Curie, Paris VI, where part of this work has been done. This work has been partially supported by the EEC-TMR Program, Contract N. CT98-0169 (EURODAΦNE).

References

- [1] J. Stern, in *Chiral Dynamics: Theory and Experiment*, eds. A.M. Bernstein, D. Drechsel and T. Walcher, Springer-Verlag, 1998, Lecture Notes in Physics 513; [hep-ph/9712438](#).
- [2] R.S. Chivukula, lectures given at Les Houches Summer School in Theoretical Physics, Les Houches, France (1998), to be published in the proceedings; [hep-ph/9803219](#).
- [3] M.E. Peskin and T. Takeuchi, *Phys. Rev. D* **46** (1992) 381;
A. Dobado, D. Espriu and M.J. Herrero, *Phys. Lett. B* **255** (1991) 405;
E. Bagan, D. Espriu and J. Manzano, [hep-ph/9809237](#).
- [4] M. Knecht and E. de Rafael, *Phys. Lett. B* **424** (1998) 335.
- [5] M. Knecht, in: V EurodaΦne Collaboration Meeting, Frascati (1997), LNF-97/021 (IR).
- [6] S. Weinberg, *Physica A* **96** (1979) 327.

- [7] J. Gasser and H. Leutwyler, *Ann. Phys. (NY)* **158** (1984) 142.
- [8] J. Gasser and H. Leutwyler, *Nucl. Phys.* **B 250** (1985) 465.
- [9] M. Gell-Mann, R.J. Oakes and B. Renner, *Phys. Rev.* **175** (1968) 2195.
- [10] N.H. Fuchs, H. Sazdjian and J. Stern, *Phys. Lett.* **B 269** (1991) 183;
J. Stern, H. Sazdjian and N.H. Fuchs, *Phys. Rev.* **D 47** (1993) 3814;
M. Knecht, B. Moussallam and J. Stern, in The Second DaΦne Physics Handbook,
eds. L. Maiani, G. Pancheri and N. Paver, 1995; [hep-ph/9411259](#).
- [11] M. Knecht, B. Moussallam, J. Stern and N. H. Fuchs, *Nucl. Phys.* **B 457** (1995) 513.
- [12] G. Ecker, *Prog. Part. Nucl. Phys.* **36** (1996) 71;
J. Stern, in Proceedings of the Workshop on Physics and Detectors for DaΦne '95,
eds. R. Baldini, F. Bossi, G. Capon and G. Pancheri, Frascati Physics Series vol. IV,
INFN-LNF SIS-Ufficio Pubblicazioni, 1995; [hep-ph/9510318](#);
M.R. Pennington, *Nucl. Phys. A Nucl. Phys.* **A 623** (1997) 189C;
H. Leutwyler, *Nucl. Phys. A Nucl. Phys.* **A 623** (1997) 169C.
- [13] J. Bijnens, G. Colangelo, G. Ecker, J. Gasser and M. Sainio, *Nucl. Phys.* **B 508**
(1997) 263.
- [14] B. Adeva et al. Lifetime measurement of $\pi^+\pi^-$ atoms to test low-energy QCD pre-
dictions, CERN/SPSLC 95-1.
- [15] J. Lowe and S. Pislak, private communication.
- [16] J. Lee-Franzini, in The Second DaΦne Physics Handbook, eds. L. Maiani, G. Pancheri
and N. Paver, 1995.
- [17] G. Colangelo, M. Finkemeier and R. Urech, *Phys. Rev.* **D 54** (1996) 4403.
- [18] M. Perl, invited talk at The Fifth International WEIN Symposium: A Conference on
Physics Beyond the Standard Model, Santa Fe, New Mexico, 1998; [hep-ph/9812400](#).
- [19] J. H. Kühn and E. Mirkes, *Z. Physik* **C 56** (1992) 661.
- [20] L. Ametller, J. Kambor, M. Knecht and P. Talavera, [hep-ph/9904452](#).
- [21] L. Girlanda, in preparation.
- [22] L. Girlanda, M. Knecht and J. Stern, in preparation.
- [23] S. M. Roy, *Phys. Lett.* **B 36** (1971) 353; *Helv. Phys. Acta* **63** (1990) 627.
- [24] D. Morgan and G. Shaw, *Nucl. Phys.* **B 10** (1969) 1387.
- [25] M. Knecht, B. Moussallam, J. Stern and N. H. Fuchs, *Nucl. Phys.* **B 471** (1996) 445.
- [26] J. Bijnens, G. Colangelo, G. Ecker, J. Gasser and M. Sainio, *Phys. Lett.* **B 374**
(1996) 210.

- [27] L. Girlanda, M. Knecht, B. Moussallam and J. Stern, *Phys. Lett.* **B 409** (1997) 461.
- [28] G. Colangelo, J. Gasser and H. Leutwyler, private communication.
- [29] L. Rosselet et al., *Phys. Rev.* **D 15** (1977) 574.
- [30] J. Bijnens, G. Colangelo and P. Talavera, *J. High Energy Phys.* **5** (1998) 14.
- [31] J. Bijnens, G. Colangelo and J. Gasser, *Nucl. Phys.* **B 427** (1994) 427.
- [32] J. Stern, N. H. Fuchs and M. Knecht, contribution to The third Workshop on the τ Charm Factory, Marbella, Spain, (1993); [hep-ph/9310299](#).
- [33] C. A. Dominguez and E. de Rafael, *Ann. Phys. (NY)* **174** (1987) 372.
- [34] J. Bijnens, J. Prades and E. de Rafael, *Phys. Lett.* **B 348** (1995) 226.
- [35] F. Guerrero and A. Pich, *Phys. Lett.* **B 412** (1997) 382.